IJISEM
INTERNATIONAL JOURNAL OF INNOVATIONS IN SCIENCE ENGINEERING AND MANAGEMENT

OPEN ACCESS

Volume: 5

Issue: 2

Month: June

Year: 2026

ISSN: 2583-7117

Published: 01.06.2026

Citation:

Mobasshir Jamal, Prof. Piyush Verma "Computational Analysis of Passive Cooling Techniques for Improving Thermal Comfort in Naturally Ventilated Classrooms" International Journal of Innovations in Science Engineering and Management, vol. 5, no. 2, 2026, pp. 353-363

DOI:

10.69968/ijisem.2026v5i2353-363

Computational Analysis of Passive Cooling Techniques for Improving Thermal Comfort in Naturally Ventilated Classrooms

Mobasshir Jamal[1], Prof. Piyush Verma[2]

[1]*Research Scholar, Corporate Institute of Science & Technology, Bhopal*

[2]*Assistant Professor, Corporate Institute of Science & Technology, Bhopal*

Abstract

By using ambient environmental factors like wind and buoyancy, natural ventilation is a successful and long-term strategy for enhancing indoor thermal comfort. This study investigates the performance of six different classroom ventilation configurations, including a roof-mounted windcatcher, variations in inlet–outlet window positions, and multiple opening arrangements. The objective is to evaluate the influence of these configurations on thermal comfort under natural airflow conditions. A cuboidal classroom model was developed based on environmental conditions representative of Madrid, Spain, and a numerical investigation was conducted using Computational Fluid Dynamics (CFD) in ANSYS fluent. The standard k–ε turbulence model coupled with the species transport model was employed to simulate airflow and pollutant dispersion. The inlet conditions were defined with an airflow velocity of 3.3 m/s and a temperature of 29 °C. Thermal comfort was assessed using average indoor temperature and heat removal effectiveness (HRE). The results indicate that airflow distribution and ventilation efficiency are highly dependent on the placement and geometry of openings. Configurations with well-defined airflow paths exhibited improved mixing and convective heat removal. Among all cases, Configuration 2 demonstrated the best performance, achieving the highest HRE of 1.946 and an average indoor temperature of 29.74 °C, indicating superior thermal comfort conditions.

Keywords; Windcatcher, Natural Ventilation, Thermal Comfort, Heat Removal Effectiveness (HRE), Computational Fluid Dynamics (CFD).

INTRODUCTION

Natural ventilation is a sustainable and indispensable approach to ensure a comfortable indoor atmosphere. It describes the method of delivering and withdrawing air without the need of mechanical devices by using natural factors like temperature variations and wind pressure. In buildings, natural ventilation is achieved through openings such as windows, doors, vents, and architectural features like windcatchers and atriums [1]. With increasing concerns over energy consumption and environmental sustainability, natural ventilation has gained significant importance as it reduces dependence on air-conditioning systems and promotes energy-efficient building design [2]. In indoor environments such as classrooms, offices, and residential spaces, proper ventilation is essential to ensure adequate air circulation and maintain indoor air quality (IAQ) [3]. The health and wellbeing of inhabitants are enhanced by natural ventilation, which helps to dilute and remove indoor pollutants such "carbon dioxide (CO2), volatile organic compounds (VOCs), and airborne particles". Furthermore, it is essential for controlling humidity and temperature, both of which have a direct impact on thermal comfort [4].

Thermal comfort is the mental condition that signifies satisfaction with the thermal surroundings in which one is located. It is affected by a variety of factors, such as "air temperature, humidity, air velocity, and radiant heat" [5]. Maintaining thermal comfort is crucial for occupant productivity, focus, and general performance in indoor workplaces, particularly in crowded areas like classrooms [6]. Poor thermal conditions can lead to discomfort, fatigue, reduced cognitive

function, and health issues such as dehydration or heat stress [7]. The need for thermal comfort in indoor environments has become increasingly important due to rising global temperatures and changing climatic conditions. The inordinate dependence on mechanical cooling systems in numerous regions results in raised greenhouse gas emissions and higher energy consumption [8]. Natural ventilation offers a viable alternative by utilizing ambient environmental conditions to provide cooling and airflow, thereby reducing energy demand while maintaining acceptable comfort levels [9], [10].

Furthermore, effective natural ventilation design ensures proper airflow distribution within the occupied zone, minimizing stagnant regions and enhancing convective heat removal. By optimizing the placement and size of openings, as well as considering building orientation and external wind conditions, it is possible to achieve both improved indoor air quality and thermal comfort [11]. In conclusion, natural ventilation is a key strategy for creating sustainable and comfortable indoor environments. Its ability to enhance air quality, regulate thermal conditions, and reduce energy consumption makes it an essential component in modern building design, particularly in educational and residential spaces where occupant comfort and health are of primary importance [12].

Thermal Comfort and the Role of Ventilation in Thermal Comfort

Thermal comfort is a state of satisfaction with the thermal environment which surrounds the occupant. It plays a vital role in the indoor environment, impacting human health, productivity, concentration and wellbeing in classrooms, offices and residential buildings [13]. The factors affecting thermal comfort are: air temperature, relative humidity, air velocity, radiant temperature, clothing insulation, and metabolic activity. The poor thermal conditions may lead to discomfort, fatigue, decrease in working capacity, dehydration and heat stress [14]. Ventilation has a significant effect on thermal comfort by controlling the flow, temperature and humidity of the indoor environment [15]. Proper ventilation brings in fresh air from the outside and expels stale air, excess heat and indoor pollutants. Openings such as windows, vents and other natural ventilation openings contribute to increased air movement and convective heat transfer contributing to cooling occupants and indoor space [16].

Ventilation is used to generate airflow which enhances the thermal sensation by increasing heat dissipation from the human body. Distributing the airflow also helps to reduce stagnant air areas and provide even temperature levels in the zone of interest. Ventilation is especially significant in hot climates since it helps to minimize the buildup of indoor heat and the need for mechanical cooling [17]. In addition, the proper design of ventilation systems can enhance indoor air quality (IAQ) by eliminating pollutants like carbon dioxide (CO_2), odors, and airborne particles, which can improve the quality of the indoor air environment. Hence, maintaining the indoor thermal comfort and supporting the wellbeing of occupants in terms of health and efficiency of work rely on proper and sustainable ventilation [18].

Role of Airflow in Maintaining Comfort in Indoor Environments

The airflow is among the most significant factors affecting indoor environment comfort and health. It is the circulation and distribution of air in a space by natural or mechanical means [19]. Thermal comfort, indoor temperature control, humidity control and indoor air quality (IAQ) depend on proper air flow. In indoor applications like classrooms, offices, and residential buildings, air flow has an important role in maintaining a comfortable and healthy environment for the occupants [20]. The main function of airflow is to control the indoor temperature. As air moves around, it will increase the heat transfer by convection, while carrying heat away from the occupants and surrounding surfaces [21]. By increasing the airflow speed, the heat transfer to the human body will be enhanced, through faster sweat evaporation, even at higher temperatures, which will make the body more comfortable. This is particularly useful in warm climatic conditions where mechanical cooling systems are not needed due to natural ventilation [22].

Another important part of the benefits of airflow is that it also helps in maintaining the quality of indoor air. Good ventilation will help to reduce and eliminate indoor air contaminants, including carbon dioxide (CO_2), volatile organic compounds (VOCs), dust particles and odors. Fresh outdoor air continuously replace stale indoor air, decrease the concentration of contaminants and minimize the risk of respiratory problems and spreading of airborne diseases [23]. Furthermore, the correct air flow avoids creation of stagnant air zones and steady heat and humidity throughout the useable space. Inadequate airflow can result in thermal non-uniformity, discomfort and decreased productivity for occupants. Thus, it is important to manage the air flow in the buildings with the proper design of ventilation system to create a healthy, comfortable and energy efficient indoor environment [24].

IJISEM
INTERNATIONAL JOURNAL OF INNOVATIONS IN SCIENCE ENGINEERING AND MANAGEMENT

OBJECTIVE

1. To study the thermal comfort inside the classroom through the natural air flow from the windcatcher.
2. To study the thermal comfort inside the classroom through the inlet and outlet window.
3. To study the variation in position of the inlet and outlet window.
4. To study the thermal comfort inside the classroom through the multiple inlet and outlet window.

RESEARCH METHODOLOGY

Governing equation

This work used "the three-dimensional Steady Reynolds Averaged Navier-Stokes (SRANS)" modeling, which is renowned for its capacity to accurately forecast the flow field within and surrounding structures. The conservation equations for mass, momentum, and energy as well as the scalar transport equation are applied as follows in steady state:

The continuity equation:

$$\nabla \cdot (\rho u) = 0 \quad \dots (1)$$

Where u is the velocity vector and ρ is the density.

Momentum conservation equation:

$$\nabla \cdot (\rho u u) = -\nabla P + \rho g + \nabla \cdot (\mu \nabla u) - \nabla \cdot \tau_t \quad \dots (2)$$

Pressure is represented by P, the gravitational acceleration vector by g, molecular dynamic viscosity by μ, and Reynolds stresses by τt.

Turbulent kinetic energy (k):

$$\nabla \cdot (\rho k u) = \nabla \cdot \left(\alpha_k \mu_{eff} \nabla k\right) + G_k + G_b - \rho\varepsilon \quad \dots (3)$$

Energy dissipation rate (ε):

$$\nabla \cdot (\rho \varepsilon u) = \nabla \cdot \left(\alpha_\varepsilon \mu_{eff} \nabla \varepsilon\right) + C_{1\varepsilon} \frac{\varepsilon}{k} (G_k + C_{3\varepsilon} G_b) - C_{2\varepsilon} \rho \frac{\varepsilon^2}{k} \quad \dots (4)$$

where the sources of turbulent kinetic energy are represented by Gk and Gb, respectively, for the average velocity gradient and buoyancy force. While C1ε, C2ε, and C3ε are empirical constants, αk and αε are the turbulent Prandtl numbers.

Energy conservation equation:

$$\nabla \cdot (\rho e u) = \nabla \cdot \left(k_{eff} \nabla T\right) - \nabla \cdot \left(\sum_i h j_i\right) \quad \dots (5)$$

Where T and e stand for temperature and specific internal energy, respectively. Effective heat conductivity is denoted by keff, while specific enthalpy is denoted by h_i.

Passive scalar transport equation:

$$\nabla \cdot (\rho c u) = \nabla \cdot \left(D_{eff} \nabla c\right) \quad \dots (6)$$

where Deff represents the effective diffusion coefficient and c stands for the constituent's concentration.

The operational temperature's maximum and lower bounds (with 80% acceptance) are as follows:

$$T_{upper}(℃) = 0.31 \times T_p(℃) + 21 \quad \dots (7)$$

$$T_{lower}(℃) = 0.31 \times T_p(℃) + 14.3 \quad \dots (8)$$

The prevailing mean outside air temperature, or Tp, is the arithmetic average of the mean daily outdoor temperatures recorded over the course of a month.

Another important statistic that can offer a deeper knowledge of passive cooling efficiency is heat removal effectiveness (HRE), a critical indicator of how well a specific ventilation technique can remove the generated heat from an enclosed area. This measure, often known as the ventilation effectiveness ratio for heat dispersion, is defined as follows:

$$HRE = \frac{T_e - T_0}{T_r - T_0} \quad \dots (9)$$

Te, To, and Tr stand for the average temperature of the air in the windcatcher exhaust, the outside air temperature, and the room's volume-averaged temperature, respectively.

Geometry and Computation domain

A cuboidal generic building was developed to represent a classroom environment with dimensions of 6 m × 6 m × 3 m (length × breadth × height). Inside the classroom, twenty students were modeled as cuboidal manikins with dimensions of 0.3 m × 0.3 m × 1.2 m to simulate seated occupants. The manikins were uniformly distributed throughout the classroom to ensure an even representation of occupancy conditions. The classroom geometry and manikin dimensions were kept constant for all six configurations, while only the ventilation arrangements were varied to investigate their influence on airflow distribution and thermal comfort.

In Configuration 1, natural ventilation was achieved using a roof-mounted windcatcher. The windcatcher had

dimensions of 0.65 m (length), 1.2 m (width), and 1.0 m (height), with a duct cross-section of 0.5 m × 0.55 m. Additionally, side wing walls with a length of 0.5 m and a deviation angle of 60° were incorporated to guide and direct airflow into the indoor space effectively. The computational domain and geometry of this configuration are illustrated in the corresponding figure.

Configuration 2 employed a simple cross-ventilation strategy using one inlet and one outlet window. The inlet opening was positioned on the front wall, while the outlet opening was located on the back wall. Both windows had identical dimensions of 5.0 m × 0.2 m, allowing direct airflow through the classroom. The computational domain and geometry of this configuration are illustrated in the corresponding figure.

In Configuration 3, one inlet window was placed on the front wall, while three outlet windows were provided to promote multidirectional airflow distribution. The inlet window measured 5.0 m × 0.2 m. Among the outlet windows, one was located on the back wall with dimensions of 3.0 m × 0.2 m, while two additional outlet windows were positioned on the side walls, each measuring 1.0 m × 0.2 m. This arrangement enhanced air extraction and circulation inside the classroom. The computational domain and geometry of this configuration are illustrated in the corresponding figure.

Configuration 4 consisted of two inlet windows located on the front wall and two outlet windows positioned on the front and back walls. Each inlet and outlet window had identical dimensions of 2.0 m × 0.25 m. This arrangement was designed to improve airflow balance and distribution within the classroom. The computational domain and geometry of this configuration are illustrated in the corresponding figure.

In Configuration 5, one inlet window with dimensions of 4.5 m × 0.3 m was provided on the front wall, while two outlet windows, each measuring 2.0 m × 0.2 m, were positioned on the front and back walls. This setup facilitated efficient airflow exchange and removal of indoor contaminants. The computational domain and geometry of this configuration are illustrated in the corresponding figure.

Configuration 6 included a single inlet and a single outlet window. The inlet window, located on the front wall, had dimensions of 5.0 m × 0.35 m, while the outlet window on the back wall measured 3.0 m × 0.2 m. This configuration represented a basic ventilation strategy with directed airflow through the occupied zone. The computational domain and geometry of this configuration are illustrated in the corresponding figure.

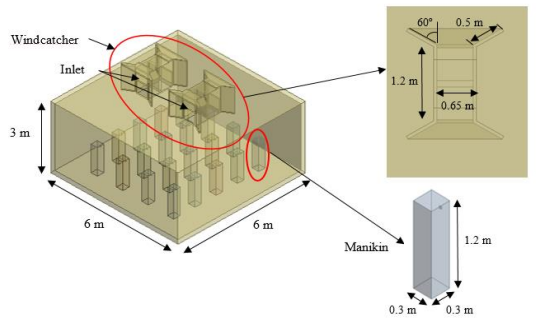

Configuration 1

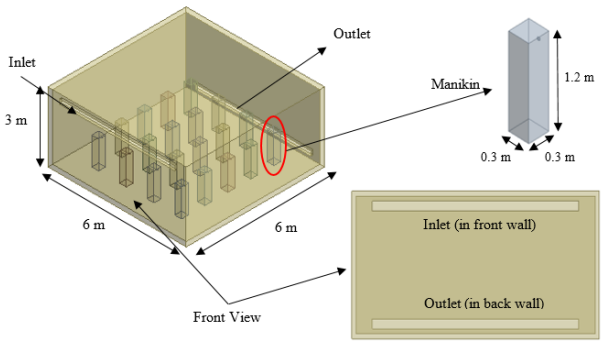

Configuration 2

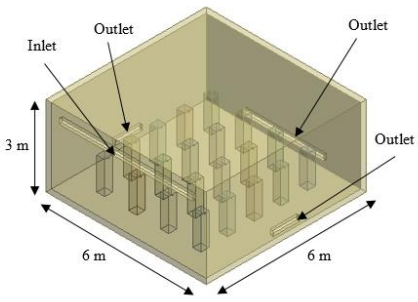

Configuration 3

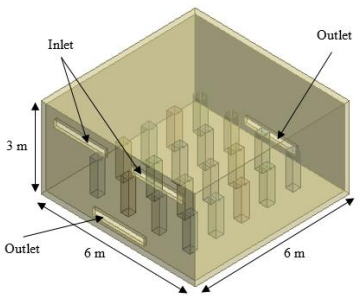

Configuration 4

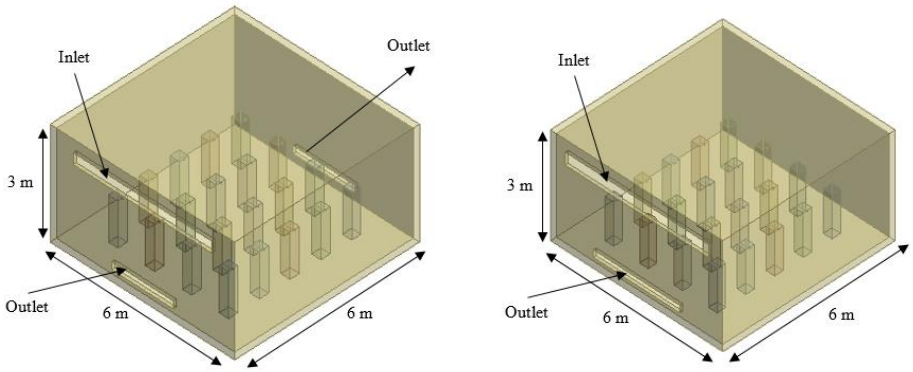

Configuration 5 Configuration 6

Figure 1: Computational domain of configuration 1-6

In this study, six cases were used to simulate the effect of natural ventilation on indoor thermal comfort in classroom environment. Each case corresponds to a distinct ventilation configuration, resulting in a total of six configurations analyzed. The details of these configurations and their corresponding cases are presented in the table.

Mesh generation

For the meshing of computational domain of class room, tetrahedral use of the element shape. There are 2 body size use for meshing one for air, and room domain which is 0.2 m and other for manikin which is 0.05 m. from the meshing the range of element are 55124 – 56403, similarly, the range of number of nodes are 249315 – 253606. The figure illustrate the meshing of computation domain of classroom.

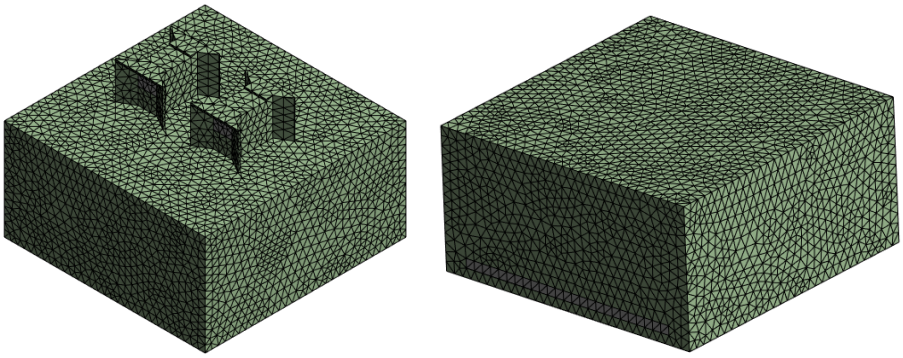

Figure 2: Meshing of computational domain of classroom

Table 1: Number of element and nodes of all configuration of classroom

Cases	Configuration	Nodes	elements
Case 1	Configuration 1 (Windcatcher-Based Ventilation)	56403	253606
Case 2	Configuration 2 (Identical Inlet and Outlet Windows)	55152	249645
Case 3	Configuration 3 (Single Inlet with Multiple Outlets)	55342	250201
Case 4	Configuration 4 (Multiple Inlets and Outlets)	55124	249315
Case 5	Configuration 5 (Single Inlet with Dual Outlets)	55174	249568
Case 6	Configuration 6 (Single Inlet–Outlet Configuration)	55201	249868

Boundary and numerical condition

The classroom model and surrounding computational domain were developed based on environmental conditions representative of Madrid, Spain. To simulate realistic outdoor airflow, profiles of vertical velocity magnitude were imposed at the inlet, representing the approaching wind conditions. A constant inlet air temperature of 29 °C, corresponding to the average daily high temperature in June, was specified. The month of June was selected for analysis as it represents the final period of the academic year and

typically experiences elevated thermal conditions. At the outlet, a zero-gauge pressure boundary condition was applied to allow free outflow of air. The upper and lateral boundaries of the computational domain were defined using symmetry boundary conditions, minimizing computational effort while maintaining flow accuracy. Gravitational acceleration was incorporated in all simulations with a value of 9.81 m/s² to account for buoyancy effects.

The standard k–ε viscous turbulence model was used for modelling the flow and dispersion of pollutants in the indoor environment together with the species transport model. All the solid surfaces were given the no-slip boundary condition, which means that no air flow was allowed to occur at the solid surfaces. The SIMPLE (Semi-Implicit Method for Pressure-Linked Equations) algorithm to couple pressure-velocity was used to obtain the numerical solution. The second order scheme was used for both pressure and energy equations for improving the accuracy of the solution. The convergence criteria for continuity, momentum (velocity), and energy equations were set to 1×10^{-6}, ensuring a high level of numerical precision.

The inlet airflow velocity was specified as 3.3 m/s, representing typical wind conditions. In addition to airflow modelling, internal heat and pollutant sources were incorporated through the manikins. Each manikin was assigned a metabolic heat generation rate of 115.76 W (equivalent to 1.3 met), which corresponds to the recommended metabolic rate for seated teenage students engaged in routine classroom activities. Furthermore, carbon dioxide (CO_2) emission was modeled through the mouth of each manikin, represented as a rectangular opening with dimensions of 0.01 m (height) × 0.013 m (width). This approach enabled realistic simulation of human respiration and its impact on indoor air quality.

Validation

The development of a computational domain and numerical modelling approach is the very important step for any study in CFD analysis that ensures reliability and accuracy of the flow behaviour prediction in the computational domain. The numerical model used in the present study has been validated by comparing with the numerical data reported by Payam Nejat et al. (2025) [20]. For the validation process, a classroom model with dimensions of 6 m × 6 m × 3 m (length × width × height) was considered. The classroom was equipped with a roof-mounted windcatcher to facilitate natural ventilation. The windcatcher dimensions were taken as 1.1 m (length), 2.1 m (width), and 1.5 m (height), with a duct cross-section of 1 m × 1 m. Additionally, the windcatcher included side wing walls of 0.5 m length with a deviation angle of 60°. The geometry and design parameters were selected based on previously validated studies to ensure consistency. Gravitational acceleration was included in the simulations with a value of 9.81 m/s² to account for buoyancy-driven flow effects. The standard k -e turbulence model was used to model the airflow patterns as well as the dispersion of pollutants. Use of no-slip boundary condition was implemented on all solid surfaces, which have zero velocity at the walls. The governing equations were solved using the SIMPLE algorithm of pressure velocity coupling. The pressure velocity coupling algorithm (SIMPLE) was used to solve the governing equations. Second-order schemes of discretization of pressure and energy equations were used to enhance numerical accuracy. The convergence criteria for all governing equations were maintained at a sufficiently low level to ensure solution stability and precision. At the inlet, a uniform airflow velocity of 3.3 m/s and a constant temperature of 29 °C were specified, representing typical environmental conditions. Internal heat generation and pollutant sources were modeled using manikins. Each manikin was assigned a metabolic heat generation rate of 115.76 W (1.3 met), corresponding to seated student activity. Carbon dioxide (CO_2) emission was introduced through the mouth of each manikin, modeled as a rectangular opening of 0.01 m × 0.013 m. The computational domain used for validation is illustrated in the corresponding figure. A comparison of temperature contours between the present simulation and the reference study (Payam Nejat et al., 2025) [20] was conducted. Additionally, the indoor air temperature distribution obtained from both studies was analyzed. The results showed a close agreement, with a maximum temperature difference of only 0.19 °C, confirming the accuracy and reliability of the present computational domain and numerical modelling approach.

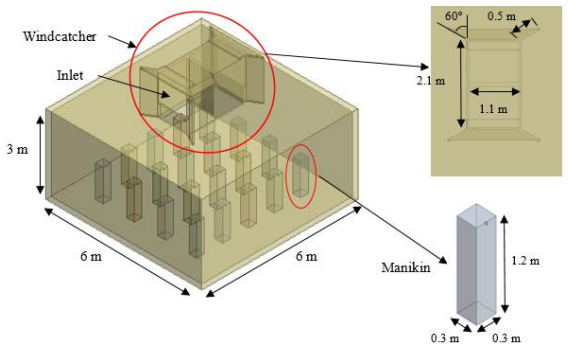

Figure 3: Geometry details of computational domain use for validation

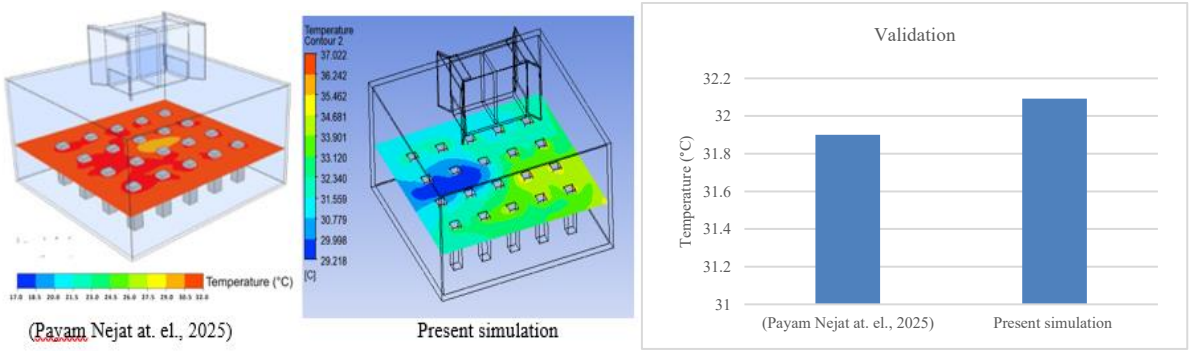

(a) (b)

Figure 4: (a) Temperature contour in validation, (b) Temperature comparison of inside the room in both result present and (Payam Nejat at. el., 2025).

RESULT AND DISCUSSION

Temperature and velocity distribution

All of the six configurations were analyzed to consider the effectiveness of various natural ventilation strategies, to achieve the thermal comfort at the breathing height of seated students. The location, the size and the number of inlet and outlet openings, the air exchange rates, the flow circulation and the efficiency of heat removed mainly determine the variations in the thermal behaviour and the airflow pattern.

In case 1, airflow is introduced through a roof-mounted windcatcher, resulting in a predominantly vertical air distribution pattern. The maximum and minimum temperatures at the breathing height were observed as 36.495 °C and 27.272 °C, respectively, with an average room temperature of 30.43 °C. The relatively higher temperature variation is attributed to non-uniform air distribution and localized recirculation zones, which limit effective heat removal in certain regions. The inlet air enters at a constant velocity of 3.3 m/s, and due to flow acceleration and redirection near solid boundaries, the velocity increases to a maximum of 5.44 m/s. This localized increase is caused by the Venturi effect and flow impingement on walls, leading to uneven airflow distribution.

In case 2, airflow enters through a continuous opening at the upper section of the front wall and exits through a similar opening at the back wall, establishing a direct cross-ventilation path. The maximum and minimum temperatures at the breathing level were 33.513 °C and 29.295 °C, respectively, with an average room temperature of 29.74 °C. The improved thermal performance compared to Configuration 1 is due to enhanced air exchange efficiency and reduced stagnation zones, allowing more uniform heat removal. The airflow maintains its maximum velocity of 3.3 m/s near the inlet region, gradually dissipating as it travels through the room due to frictional and turbulent effects.

Case 3 incorporates one inlet and three outlet openings, promoting multi-directional airflow distribution. The maximum and minimum temperatures at the breathing height were 33.157 °C and 29.356 °C, respectively, with an average temperature of 29.78 °C. The presence of multiple outlets improves air extraction efficiency and reduces thermal stratification; however, slight temperature variations persist due to uneven flow partitioning among the outlets. The inlet velocity remains at 3.3 m/s, with peak velocity observed at the entry region.

In case 4, two inlet and two outlet windows are provided, creating a more distributed airflow network. The maximum and minimum temperatures recorded were 33.644 °C and 29.367 °C, respectively, with an average room temperature of 29.83 °C. Although multiple openings enhance airflow distribution, the thermal performance is slightly lower than Configuration 3 due to interference between airflow streams and potential short-circuiting of air, where fresh air exits before effectively mixing within the occupied zone.

In the case of maximum temperature of 32.608 °C and minimum temperature of 29.243 °C, the average temperature of the room is 29.69 °C as shown in case 5. This improvement is attributed to a balanced inlet–outlet area ratio and optimized airflow path, which enhances convective heat removal and reduces localized heat accumulation. The airflow enters at 3.3 m/s and maintains higher momentum within the occupied zone, improving thermal comfort.

Case 6 shows the best thermal performance in all of the cases with maximum temperature of 31.44 °C, and minimum temperature of 29.222 °C at the breathing height. The average room temperature is 29.56 °C, indicating the

most uniform thermal distribution. The improved performance is due to a well-defined airflow path, reduced recirculation zones, and efficient removal of warm air from the occupied region. The single inlet and outlet arrangement minimizes flow disturbances and ensures steady and uniform air movement, resulting in better heat dissipation.

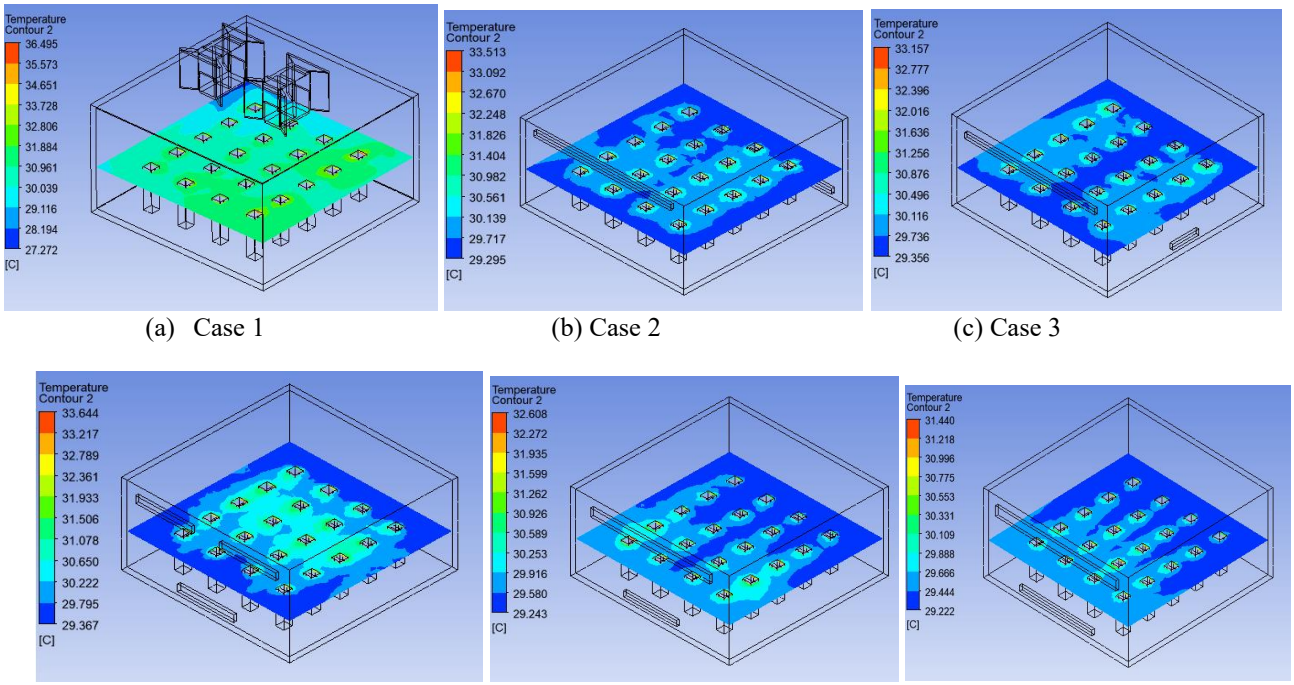

(a) Case 1 (b) Case 2 (c) Case 3

(d) Case 4 (e) Case 5 (f) Case 6

Figure 5: Temperature contour in case 1-6

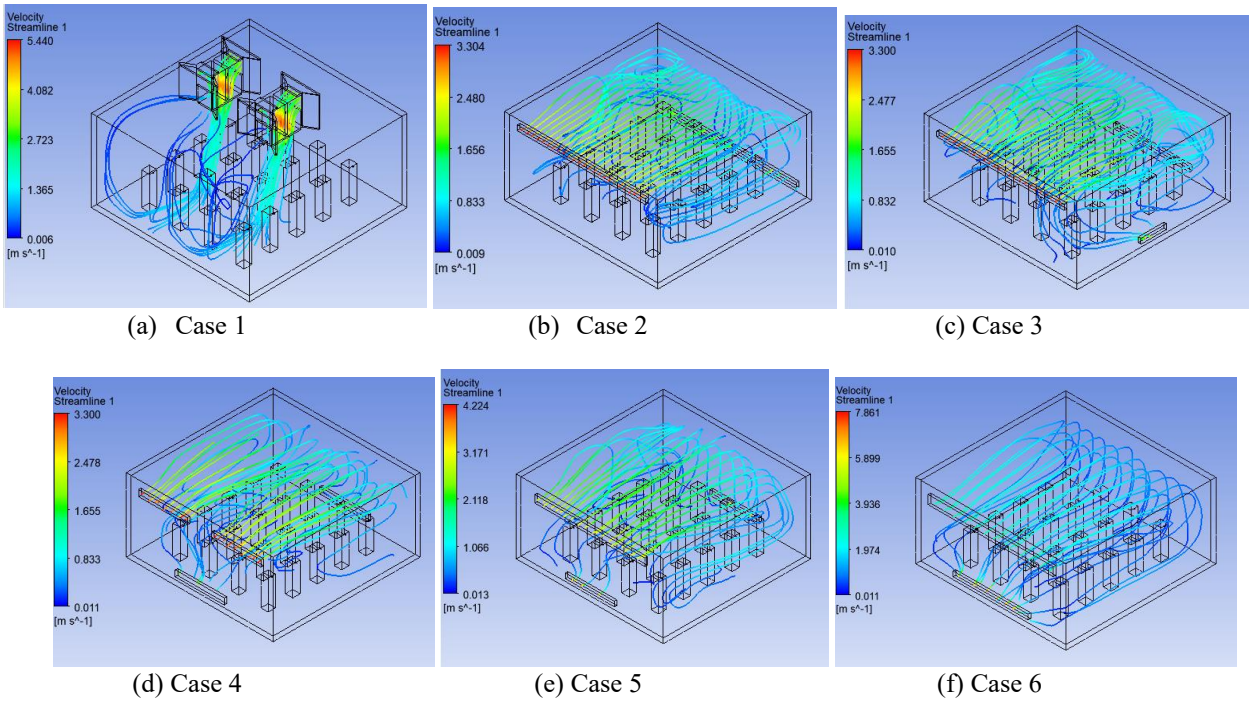

(a) Case 1 (b) Case 2 (c) Case 3

(d) Case 4 (e) Case 5 (f) Case 6

Figure 6: Velocity contour in case 1-6

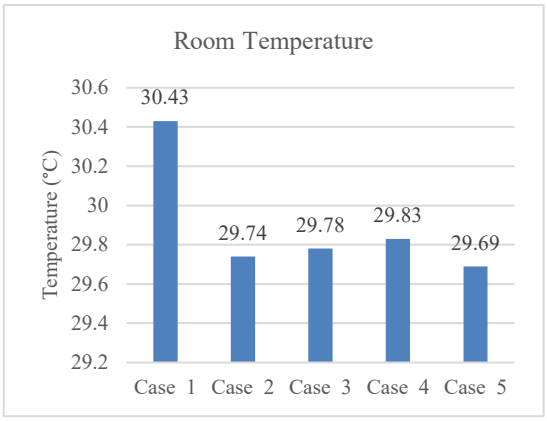

Figure 7: Average Room temperature in all cases

Heat removal effectiveness (HRE)

The Heat Removal Effectiveness (HRE) also known as the ventilation effectiveness ratio is a very important parameter used to determine the performance of a natural ventilation system in terms of its effectiveness in removing internally generated heat to an enclosed space. It gives a quantitative estimate of the effectiveness of a ventilation strategy to remove thermal loads in occupied space as compared to the given air conditions. Higher HRE values indicate more effective heat removal and improved cooling performance. In the present study, the HRE values for the six configurations were found to be 0.768, 1.946, 1.856, 1.716, 1.676, and 1.572 for Configuration 1 through Configuration 6, respectively. Correspondingly, the average indoor temperatures were 30.43 °C, 29.74 °C, 29.78 °C, 29.83 °C, 29.69 °C, and 29.56 °C.

In Configuration 1 (windcatcher-based ventilation), the lowest HRE value (0.768) was observed, despite moderate airflow velocities. This is mainly because of the non-uniform vertical airflow distribution, local recirculation zones and the inefficient removal of warm air from the occupied zone. Therefore, the indoor temperature of the classroom is heated up, and the classroom has the highest average indoor temperature (30.43 °C) of all cases.

In Configuration 2 (single inlet–outlet cross ventilation), the highest HRE value (1.946) was achieved. This superior performance is attributed to a well-defined and unidirectional airflow path, which enhances convective heat transfer and ensures efficient removal of warm air from the breathing zone. The strong cross-ventilation minimizes stagnation zones and promotes effective air exchange, resulting in a relatively lower average temperature (29.74 °C).

Configuration 3 (single inlet with multiple outlets) also demonstrates high HRE (1.856), slightly lower than Configuration 2. The presence of multiple outlets improves air extraction capacity and reduces thermal stratification. However, unequal flow distribution among outlets and minor flow disturbances lead to a marginal reduction in heat removal efficiency compared to Configuration 2.

In Configuration 4 (multiple inlets and outlets), the HRE value decreases to 1.716. Although multiple openings enhance airflow availability, the performance is affected by airflow interference, turbulence interactions, and possible short-circuiting, where incoming fresh air exits prematurely without effectively mixing with indoor air. This results in slightly higher average temperatures (29.83 °C).

Configuration 5 (optimized inlet–outlet arrangement) exhibits an HRE of 1.676, with improved thermal performance compared to Configuration 4. The relatively balanced inlet–outlet configuration enhances air mixing and convective heat removal, leading to a reduced average indoor temperature (29.69 °C). However, the slightly lower HRE compared to Configurations 2 and 3 suggests that airflow is not fully optimized for maximum heat extraction.

In Configuration 6 (basic inlet–outlet configuration), the HRE value is 1.572, which is lower than Configurations 2–5 but still significantly higher than Configuration 1. Despite this, Configuration 6 achieves the lowest average indoor temperature (29.56 °C). This can be attributed to a stable and uniform airflow pattern, minimal recirculation zones, and effective cooling of the occupied region, even though the overall heat removal rate is comparatively moderate.

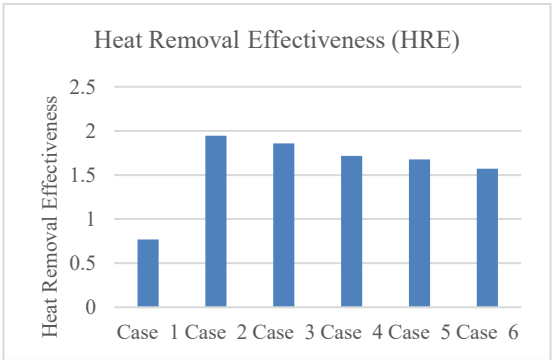

Figure 8: Heat Removal effectiveness in all cases

While Configuration 2 demonstrates the highest heat removal effectiveness due to efficient cross-ventilation and strong convective heat transfer, Configuration 6 achieves the lowest average indoor temperature due to uniform airflow

distribution and stable thermal conditions within the occupied zone. On the other hand, Configuration 1 shows the least effective performance due to poor airflow distribution and limited heat extraction capability.

CONCLUSION

This present study aimed to examine the performance of six different natural ventilation arrangements in a classroom setting, with respect to temperature distribution, airflow (velocity) characteristics and heat removal effectiveness (HRE). The analysis was carried out to evaluate how variations in inlet–outlet arrangements influence indoor thermal comfort and cooling performance at the breathing height of seated occupants. From the temperature distribution results, it was observed that configurations with well-defined airflow paths and efficient air exchange exhibited lower average indoor temperatures. Configuration 1, which employed a roof-mounted windcatcher, exhibited the highest average temperature (30.43 °C) due to non-uniform airflow distribution, vertical flow dominance, and recirculation zones that reduced effective heat removal. It also showed the lowest heat removal effectiveness (HRE) of 0.768, indicating poor cooling performance. In contrast, Configurations 2–6, based on window-driven ventilation, achieved improved thermal conditions with average temperatures ranging from 29.56 °C to 29.83 °C. These configurations provided more uniform airflow distribution and better utilization of the inlet velocity (3.3 m/s), enhancing convective heat transfer and reducing stagnation zones. From the numerical study it concluded that:

1. The velocity contour analysis revealed that airflow behavior is strongly dependent on the placement and geometry of openings.
2. The variation in HRE is primarily attributed to airflow path clarity, mixing efficiency, and inlet–outlet configuration, where well-aligned openings enhance heat removal through effective convective transport.
3. In comparison of all cases, case 2 shows the effective value of heat removal effectiveness of 1.946, average room temperature of 29.74 °C.

The superior performance of Configuration 2 is due to its straightforward cross-ventilation mechanism, which ensures efficient heat removal, and minimal temperature inside the classroom.

References

[1] M. I. Abdelhady, M. I. A. Habba, M. A. Alsaber, and A. A. E. Fahmi, “CFD and site analysis for optimizing indoor air quality in sustainable social housing via windcatcher integration,” *Sci. Rep.*, vol. 16, no. 9684, pp. 1–25, 2026.

[2] Q. Ma, G. Qian, M. Yu, L. Li, and X. Wei, “Performance of Windcatchers in Improving Indoor Air Quality, Thermal Comfort, and Energy Efficiency: A Review,” *Sustainability*, vol. 16, no. 9039, pp. 1–26, 2024.

[3] K. Rana, “Towards Passive Design Strategies for in a Naturally Comfort Performance Improving Thermal Ventilated Residence,” *J. Sustain. Archit. Civ. Eng.*, vol. 2, no. 29, pp. 150–174, 2021, doi: 10.5755/j01.sace.29.2.29256.

[4] E. Kusi, I. Boateng, H. Danso, E. Appiah-kubi, F. Gyimah, and C. Barajei, “Effect of Airflow on Thermal Comfort in a Naturally Ventilated University Classroom,” *MSI J. Multidiscip. Res.*, pp. 6–30, 2025.

[5] M. Bittar, A. L. de Araujo, O. de Almeida, T. Martins, and M. Sousa, “Enhancing indoor airflow: insights on cross ventilation through CFD simulations,” *Ambient. Construído, Porto Alegre*, vol. 25, pp. 1–16, 2025.

[6] Azmatullah, B. Suresh, and S. Singh, “Examine Thermal Comfort Inside The Indoor Swimming Pool Through Various Configuration of Inlet and Outlet Vents,” *Int. J. Innov. Sci. Eng. Manag.*, vol. 4, no. 1, pp. 46–55, 2025, doi: 10.69968/ijisem.2025v4i146-55.

[7] J. A. Akubue and C. Ukpabia, “CFD MODELING OF AIRFLOW FOR IMPROVING THERMAL COMFORT IN NATURALLY VENTILATED CLASSROOM WITHIN ABUJA.,” *Open Journals Environ. Res.*, vol. 6, no. 1, pp. 44–60, 2025, doi: 10.52417/ojer.v6i1.854.

[8] R. S. Qataya, M. A. A. Mohamed, H. Alshanwany, and S. Sabbour, “A Framework for Enhancing Natural Ventilation in Hot-Arid Regions: A Bioclimatic Design Approach,” *Egypt. Int. J. Eng. Sci. Technol.*, vol. 46, pp. 39–52, 2024, doi: 10.21608/EIJEST.2023.209023.1225.

[9] I. Sarna and J. Ferdyn-Grygierek, “Natural ventilation for thermal comfort: a simulation-based comparison of manual and automated window control strategies in temperate climate housing,” *Build. Environ.*, vol. 285, no. 113551, pp. 1–19, 2025, doi: 10.1016/j.buildenv.2025.113551.

[10] A. Chourey, P. K. Verma, and P. Shrivastava,

"Thermal Comfort Analysis in Dormitory Room by Combined MVHR-Fan Coil," *Int. J. Innov. Sci. Eng. Manag.*, vol. 4, no. 3, pp. 351–363, 2025, doi: 10.69968/ijisem.2025v4i3351-363.

[11] M. T. Aguilar-carrasco, R. M. López-lovillo, R. Suárez, and Á. L. León-rodríguez, "Ventilation Strategies to Ensure Thermal Comfort for Users in School Buildings: A Critical Review," *Appl. Sci.*, vol. 15, no. 5449, pp. 1–24, 2025.

[12] I. Alhindawi, J. A. Mcgrath, D. Sood, J. O. Donnell, and M. A. Byrne, "A seasonal assessment of indoor air quality and thermal performance in naturally ventilated airtight energy-efficient dwellings," *Build. Environ.*, vol. 276, no. 112862, pp. 1–13, 2025, doi: 10.1016/j.buildenv.2025.112862.

[13] A. Ragab, M. M. Hassieb, and A. F. Mohamed, "Exploring the impact of window design and ventilation strategies on air quality and thermal comfort in arid educational buildings," *Sci. Rep.*, vol. 15, no. 19596, pp. 1–21, 2025.

[14] N. Izadyar, W. Miller, B. Rismanchi, V. Garcia-hansen, and S. Matour, "Balcony design and surrounding constructions effects on natural ventilation performance and thermal comfort using CFD simulation: a case study," *J. Build. Perform. Simul.*, vol. 16, no. 5, pp. 537–556, 2023, doi: 10.1080/19401493.2023.2185682.

[15] J. Kim, H. Naganathan, S. Moon, and D. Jang, "Optimizing Comfort and Sustainability: The Impact of Passive Cooling and Eco-Friendly Materials on Indoor Temperature Reduction—A Case Study," *Buildings*, vol. 14, no. 3218, pp. 1–21, 2024.

[16] E. Conceição, J. Gomes, M. I. Conceição, M. Conceição, M. M. Lúcio, and and H. Awbi, "Modelling of Indoor Air Quality and Thermal Comfort in Passive Buildings Subjected to External Warm Climate Conditions," *Atmosphere (Basel).*, vol. 15, no. 1282, 2024.

[17] R. Escandón, S. Ferrari, R. Cardelli, T. Blázquez, and R. Suárez, "How Do Natural Ventilation Strategies Affect Thermal Comfort in Educational Buildings? A Comparative Analysis in the Mediterranean Climate," *Appl. Sci.*, vol. 15, no. 6606, pp. 1–16, 2025.

[18] S. H. Alhmoud and H. H. Alhmoud, "Analysis of Thermal Comfort Techniques for the Performance Conserving of Buildings and Interior Spaces," *Int. J. Sustain. Dev. Plan.*, vol. 19, no. 11, pp. 4193–4201, 2024.

[19] D. Sekartaji, Y. Ryu, and D. Novianto, "Effect of ventilation patterns on indoor thermal comfort and air-conditioning cooling and heating load using simulation," *City Built Environ.*, vol. 1, no. 14, pp. 1–24, 2023, doi: 10.1007/s44213-023-00015-y.

[20] P. Nejat, Y. Fekri, M. H. Pourghasemian, H. Alsaad, and C. Voelker, "Passive cooling assessment of natural ventilation by windcatchers for enhancing thermal comfort and indoor air quality in European schools," *Build. Environ.*, vol. 276, 2025.

[21] A. M. Bello, A. Umar, I. A. Abdul, M. A. Ibrahim, M. M. Bello, and M. A. Ibrahim, "Integration of Passive Cooling Strategies for the Design of Sustainable Faculty of Architecture at Abubakar Tafawa Balewa University, Bauchi - A Review," *Int. J. Adv. Res. Soc. Sci. Environ. Stud. Technol.*, vol. 9, no. 1, pp. 148–154, 2025, doi: 10.48028/iiprds/ijarssest.v9.i1.12.

[22] K. Dharmasastha, D. G. L. Samuel, S. M. S. Nagendra, and M. P. Maiya, "Impact of indoor heat load and natural ventilation on thermal comfort of radiant cooling system: An experimental study," *Energy Built Environ.*, vol. 4, pp. 543–556, 2023, doi: 10.1016/j.enbenv.2022.04.003.

[23] C. Yetiş and M. T. Kayılı, "Improving Indoor Air Quality with Natural Ventilation Methods: A Simulation Study," *Int. J. Archit. Plan.*, vol. 12, no. 1, pp. 1–23, 2024, doi: 10.15320/ICONARP.2024.273.

[24] B. Naili, I. Háber, and I. Kistelegdi, "Natural ventilation in high-rise office building – Comfort and energy performance," *Pollack Period. An Int. J. Eng. Inf. Sci.*, vol. 18, no. 3, pp. 52–57, 2023, doi: 10.1556/606.2023.00839.